Biosensors and Bioelectronics 143 (2019) 111598

Contents lists available at ScienceDirect

Biosensors and Bioelectronics

journal homepage: www.elsevier.com/locate/bios

Nicotinamide adenine dinucleotide immobilized tungsten trioxide nanoparticles for simultaneous sensing of norepinephrine, melatonin and nicotine

A.C. Anithaa[a], K. Asokan[b], N. Lavanya[a], C. Sekar[a,*]

[a] Dept. of Bioelectronics and Biosensors, Alagappa University, Karaikudi, 630003, TN, India
[b] Materials Science Division, Inter-University Accelerator Centre, New Delhi, 110067, India

ARTICLE INFO

Keywords:
Norepinephrine
Melatonin
Nicotine
WO_3
Nicotinamide adenine dinucleotide
Electrochemical biosensor

ABSTRACT

Herein, we report the anionic surfactant, ethylene diamine tetraacetic acid (EDTA), mediated synthesis of WO_3 nanoparticles and its subsequent modification through gamma irradiation (GI) and electrochemical immobilization with nicotinamide adenine dinucleotide (NAD). Glassy carbon electrode (GCE) modified with GI-WO_3 NPs and the enzyme NAD exhibited strong electro-oxidation of three important biomolecules such as norepinephrine (NEP), melatonin (MEL) and nicotine (NIC) in 0.1 M phosphate buffer saline (PBS) at physiological pH of 7. Square wave voltammetry (SWV) studies exhibited three well-defined peaks at potentials of 120, 570 and 840 mV, corresponding to the oxidation of NEP, MEL and NIC respectively, indicating that simultaneous determination of these compounds is feasible at the NAD/GI EDTA-WO_3/GCE. The proposed sensor displayed a wide linear range of 0.010–1000 μM with the lowest detection limit of 1.4 nM for NEP, 2.6 nM for MEL and 1.7 nM for NIC respectively. Furthermore, the modified electrode was successfully applied to detect NEP, MEL and NIC in pharmaceutical and cigarette samples with excellent selectivity and reproducibility.

1. Introduction

Norepinephrine (NEP), melatonin (MEL) and nicotine (NIC) are important biomolecules that coexist in the extracellular fluid of the central nervous system and plasma. NEP (4-[(1R)-2-amino-1-hydroxyethyl] benzene-1,2-diol) is a vital catecholamine neurotransmitter, secreted and released by the adrenal glands, noradrenergic neurons and cerebral cortex (Goyal et al., 2011). NEP is responsible for increased heart rate, attention and focus, dilation of pupil and vasoconstriction. It also promotes the conversion of glycogen to glucose in the liver and helps in converting the fats into fatty acids, resulting in an increment in energy production (Samdani et al., 2016). Extreme abnormalities of NEP concentration levels may lead to thyroid hormone deficiency, congestive heart failure, arrhythmia, ganglia neuroblastoma and Parkinson's disease (Ardakani et al., 2010; Wang et al., 2015).

Melatonin (N-acetyl-5-methoxytriptamine), a methoxyindole hormone secreted by the mammalian pineal gland located deep in the brain, plays a crucial role in regulating the sleep-wake cycle and biological circadian rhythm (Kumar et al., 2016). The circadian rhythm of MEL is controlled by the suprachiasmatic nucleus that regulates the amount of NEP release from the sympathetic nerve terminals which interacts with the β-adrenoceptors leading to formation of MEL (Meng et al., 2012). MEL is responsible for a variety of physiological and behavioral processes including neurological, psychiatric, reproductive and as neuroprotective agent in Alzheimer and Parkinson's disease models (Levent, 2012).

Nicotine (3-[(2S)-1-methylpyrrolidin-2-yl]pyridine) is an alkaloid substance primarily found in various plants and a highly tobacco-specific compound in cigarette smoke which gets readily absorbed by the human body and affects broad diseases (Vargas et al., 2013). Despite its high toxicity, it has been also associated with neurodegenerative treatments, such as Alzheimer's, Parkinson's, pulmonary, and vascular diseases (Lee et al., 2018). NIC also activates and interacts with the neurotrophins in the central nervous system, facilitating the release of neurotransmitters like dopamine, serotonin, epinephrine, NEP, acetylcholine and replenishing the neurohormone stores (Akhtar et al., 2018). Due to the clinical significance of NEP, MEL and NIC, it is essential to develop an analytical method, which would be helpful to diagnose and understand the biological relationship between them consequently opening new range of clinical and pharmaceutical applications.

Over the past decades, there has been considerable interest in the

* Corresponding author.
E-mail address: Sekar2025@gmail.com (C. Sekar).

https://doi.org/10.1016/j.bios.2019.111598
Received 31 July 2019; Received in revised form 10 August 2019; Accepted 13 August 2019
Available online 16 August 2019
0956-5663/

development of methods for the determination of biomolecules by spectrofluorimetry, HPLC, capillary electrophoresis and potentiometry techniques (Thomas et al., 2015; Yasuda et al., 2013). Among these, electroanalytical sensing methods have several advantages such as low detection limit, less interference, low cost, fast response and being suitable for analytical applications. In this work, we introduce a sensitive and selective electrochemical procedure for the simultaneous determination of NEP, MEL and NIC using NAD immobilization on gamma irradiated tungsten trioxide nanoparticles (WO_3) modified glassy carbon electrode (GCE). The nicotinamides are an important class of pyridine nucleotides that functions as an oxidative cofactor in eukaryotic cells and also the coenzyme form of the vitamin niacin. The NAD coenzyme acts as a hydrogen acceptor and electron carrier in oxidation-reduction reactions in cell metabolism. Under physiological conditions, it plays a key role as redox agent that catalyzes reactions in which NAD^+ is reduced to NADH and vice versa which is responsible for the energy production through redox reactions in cellular respiration (Ali et al., 2011). Electro-deposition of NAD immobilization on WO_3 NPs was an important step for the detection of NEP, MEL and NIC. WO_3 NPs with its unique properties including optical tunable band gap, quantum confinement and structural flexibility is widely applied for the electrochemical determination of dopamine (Anithaa et al., 2015), serotonin (Anithaa et al., 2017a), epinephrine and xanthine (Anithaa et al., 2017b), guanine (Anithaa et al., 2017c) and acetylcholine (Anithaa et al., 2018). Anionic surfactants (ethylene diamine tetra-acetic acid, EDTA) have been widely used in chemistry particularly affecting several electrochemical processes, as well as in the synthesis of inorganic semiconductors. WO_3 NPs interact with EDTA through surface adsorption and proved to be useful for the determination of biological compounds. Gamma irradiation on WO_3 NPs plays a crucial role on defect creation in the form of lattice defects, vacancies, defect clusters and dislocations which acts as trapping centers for NAD immobilization.

To the best of our knowledge, no study has been published so far reporting the simultaneous determination of NEP, MEL and NIC by using any kind of modified electrodes. The aim of the present work is to construct a novel biosensor for the determination of analytes in the commercial and real samples with satisfactory recoveries.

2. Experimental

2.1. Reagents

Norepinephrine, melatonin, nicotine and nicotinamide adenine dinucleotide were purchased from Aldrich. Tungstic acid, ethylene diamine tetra acetic acid and 0.1 N sodium hydroxide solutions were purchased from Fischer Scientific. 0.1 M phosphate buffer saline (PBS) with different pH values were prepared by mixing the stock standard solutions of Na_2HPO_4 and NaH_2PO_4 and adjusting pH with 0.1 M H_3PO_4 or NaOH.

2.2. Apparatus

Powder X-ray diffraction (XRD) patterns, photoluminescence (PL), scanning electron microscopy (SEM) and X-ray photoelectron spectroscopy (XPS) were used to analyze the structural, optical, morphological properties and chemical states of pristine WO_3 in comparison with the GI WO_3 NPs. The detailed experimental conditions and instrumental information were mentioned in supplementary S1. Electrochemical measurements were executed on a CHI 609D workstation connected to glassy carbon electrodes (GCE) as the working electrode, platinum wire as counter electrode and Ag/AgCl as reference electrode.

2.3. Synthesis of WO_3 nanoparticles

The sodium tungstate solution was obtained by dissolving of tungstic acid (H_2WO_4) in sodium hydroxide (NaOH) solution. Subsequently 0.5 g of EDTA was added to the precursor solution to act as a surfactant. The final solution was exposed to microwave under optimum power of 180 W for 15 min and dried at 100 °C for an hour. The resultant products were irradiated using Gamma Chamber 1200 (1.25 MeV ^{60}Co source) at IUAC, New Delhi. WO_3 NPs were exposed to the optimized dosage of 150 kGy at room temperature and the activity at the time of exposure was 5.499 kGy/hr. The above gamma irradiation process was repeated under identical conditions for WO_3 NPs prepared with and without EDTA addition.

2.4. Preparation of modified electrodes

Prior to modification, the GCEs were first polished with sand paper followed by 1.0, 0.3, and 0.05 mm alumina slurry, respectively, and sequentially sonicated for 1 min in ethanol and double-distilled water bath to remove any residues. The procedure for the construction of the biosensor was as follows: firstly, the pretreated GCE surface was modified by dropping 10 µL of 5 mg/mL GI EDTA-WO_3 NPs suspension and dried in air for overnight at room temperature in the absence of light to form GI EDTA-WO_3/GCE. The fabricated electrode was cycled in 0.1 M H_2SO_4 solution containing 0.2 mM NAD between the potential ranges of 0.2 to −0.4 V. Subsequently, the electrode was thoroughly rinsed with double-distilled water and then dried at 4 °C for 1 h in the absence of light (denoted as NAD/**GI EDTA-WO_3**/GCE). For comparison, NAD/EDTA-WO_3/GCE and EDTA-WO_3/GCE were prepared by the similar procedure. When not in use, the electrodes were stored in aqueous solution of 0.1 M PBS (pH 7.0) at 4 °C. The storage stability and detection mechanisms can be improved through immobilization of the mediators by covalent conjugation method, which permits the most stable immobilization of both the enzymes and apatmers (Alejandra et al., 2016).

2.5. Real samples preparation

The NEP injection was diluted 100 times using deionised water and 100 µL of this solution was added to 0.1 M PBS (pH 7.0), and measured by SWV for five times. The average result of NEP in the injection was 0.98 mg/mL, which was quite consistent with that of prescribed injection specification (1.00 mg/mL). Ten melatonin tablets were weighed and ground into a fine powder. Then, 100 mg of powdered tablets was weighed, transferred to 10 mL calibrated flask and completed to the volume with de-ionized water. It was centrifuged for 15 min at 4000 rpm to complete dissolution and the mixture was filtered through a filter paper. Cigarettes were taken out of their rolling paper and dried at 40 °C in a oven for 30 min before weighing. A mixture of ten cigarettes taken from two packs of the same brand was dispersed (0.1 g) with 10 mL water, sonicated for 3 h and then filtered. 100 µL of the clear filtrate was mixed with the PBS (pH 7.0) containing 1.0 mM SDS and analyzed under same conditions.

3. Results and discussion

3.1. Physical characterization of pristine and GI EDTA-WO_3 NPs

XPS spectra were recorded to investigate the surface composition and chemical states of the pristine and GI EDTA-WO_3 NPs. It can be seen from the survey analysis shown in Fig. S1A that the W and O were the main constituent elements and carbon (C 1s) appearing at 284 eV may be due to inadvertent species from the instrument (Yang et al., 2015). Fig. 1A and B shows the corresponding tungsten (W 4f) and oxygen (O 1s) peaks for both the pristine and GI EDTA-WO_3 NPs. W 4f can be deconvoluted into a doublet with binding energy peaks at 35.44 eV and 37.58 eV, corresponding to the emission of W $4f_{7/2}$ and W $4f_{5/2}$ core-levels that belong to the W^{6+} oxidation (Zhang et al., 2015) with a spin-orbit separation of 2 eV. For GI EDTA-WO_3 NPs, the

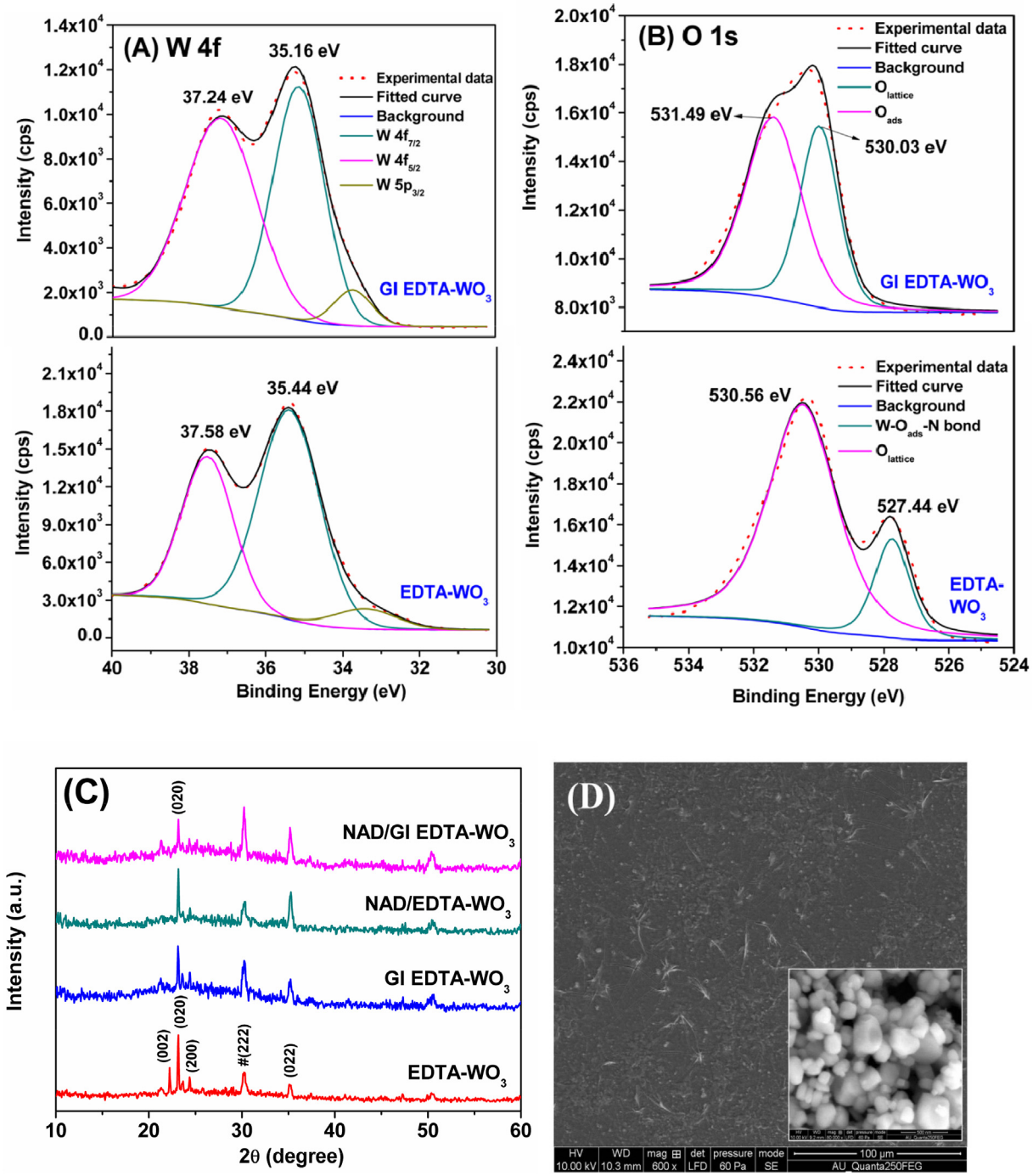

Fig. 1. XPS spectra of the pristine EDTA-WO_3 and GI EDTA-WO_3 NPs for W 4f (A) and O 1s (B) spectrum; Powder XRD patterns (C) of the pristine and GI EDTA-WO_3 with and without NAD; FESEM images (D) of NAD/GI EDTA-WO_3 with GI EDTA-WO_3 as inset.

characteristic peaks are shifted by about 0.3 eV to a lower binding energy (35.16 eV and 37.24 eV), inferring that there is no significant variation in the oxidation state of W atoms.

The O 1s spectrum shown in Fig. 1B displays the obvious peaks at 530.03 eV ascribed to lattice oxygen atoms (O^{2-}) that form the strong W = O bonds and the adsorbed oxygen (O^- and O_2^-) forms W–O bond at 531.49 eV (Wang et al., 2016) as in the case of GI EDTA-WO_3 NPs. Unlike pristine, lattice O^{2-} up-shifted to 530.56 eV, and a new peak at 527.44 eV could be attributed to W–O–N bond. According to Fig. 1B, the GI EDTA-WO_3 NPs displays significantly more adsorbed oxygen than in EDTA-WO_3 NPs, suggesting a prominent interaction of ion-adsorbed oxygen with NAD via electro-deposition.

In order to confirm the electro-deposition of NAD, the immobilization was made on WO_3 NPs/ITO; they are characterized by powder XRD, PL and FESEM. Fig. 1C shows the powder XRD patterns of pristine and GI EDTA-WO_3 NPs before and after NAD deposition. The diffraction peaks of all the samples could be well indexed to a monoclinic structure (File No. 72–0677). However, the peak intensity decreases significantly and lattice parameters changes for NAD/GI EDTA-WO_3 when compared to that of NAD free GI EDTA-WO_3 which indicate the decrement in crystallinity of WO_3 due to electro-deposition of NAD.

XRD results were further confirmed by PL spectra (Fig. S1B) through the appearance of lower intensity peaks which could be attributed to the creation of more oxygen vacancies or defects, resulting in more

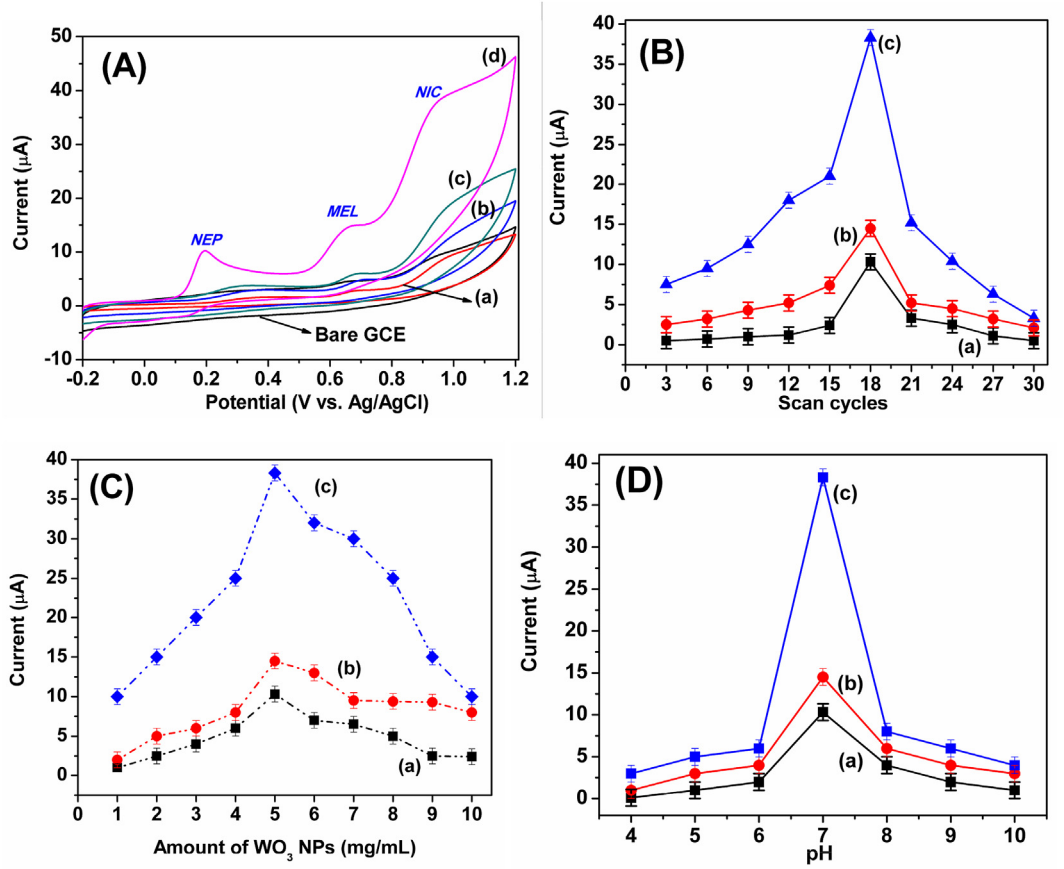

Fig. 2. CVs recorded for the simultaneous detection (A) of NEP, MEL and NIC at bare GCE, EDTA-WO_3/GCE (curve a), GI EDTA-WO_3/GCE (curve b), NAD/EDTA-WO_3/GCE (curve c) and NAD/GI EDTA-WO_3/GCE (curve d) in 0.1 M PBS (pH 7.0) at the scan rate of 50 mV/s; (B) CVs of various scan cycles for the immobilization of NAD on GI EDTA-WO_3/GCE for NEP (a), MEL (b) and NIC (c) with RSDs of 0.55%, 0.65% and 0.61% respectively; (C) CVs of varying amount of WO_3 NPs on NAD/GCE for NEP (a), MEL (b) and NIC (c) with RSDs of 0.87%, 0.95% and 0.77% respectively; (D) Plot of oxidation peak current vs. pH in 0.1 M PBS with RSDs of 1.04% (NEP, curve a), 1.15% (MEL, curve b) and 1.07% (NIC, curve c).

oxygen adsorption on the surface of the NAD/GI EDTA-WO_3 NPs. The results suggest that the modified electrode act as strong acceptors to capture the free electrons.

Fig. 1D shows FESEM images of the GI EDTA-WO_3 NPs before and after NAD electro-deposition. The NAD immobilized GI EDTA-WO_3 NPs exhibits the wrinkle shaped morphology suggesting the presence of high-density edges with electrostatic interactions between NAD and WO_3, whereas, GI EDTA-WO_3 displays the aggregated particles in the form of cuboids (Inset of Fig. 1D). It can be further explained by the migration of large amount of WO_3 particles due to the surface and adsorption of NAD on the oxide films surface. The parallelogram-shaped pristine EDTA-WO_3 NPs (Fig. S2A) changes to wavy morphology after the deposition of NAD (Fig. S2B). EDX confirms the presence of NAD on prepared WO_3 NPs with the presence of N and S atoms (Fig. S3).

3.2. Electrochemical behaviours of NEP, MEL and NIC at NAD/GI EDTA-WO_3

Fig. 2A shows the CVs recorded at various electrodes in a ternary mixture solution of 5 μM NEP, 25 μM MEL and 50 μM NIC in 0.1 M PBS (pH 7.0). At bare GCE, pristine EDTA-WO_3/GCE and gamma irradiated EDTA-WO_3/GCE, only a broad and overlapped oxidation peak was obtained and the potentials of NEP, MEL and NIC were indistinguishable to the extent that the simultaneous determination of these biological molecules was impossible. However, at the NAD immobilized GI EDTA-WO_3/GCE, three sharp and well-defined oxidation peaks with larger peak separation potential and higher peak currents corresponding to the oxidation of NEP, MEL and NIC have appeared. The three oxidation peaks for NEP, MEL and NIC are well resolved at 200, 650 and 900 mV respectively, with the peak separation potentials of 450 mV (NEP-MEL) and 250 mV (MEL-NIC). All the observed voltammetric responses demonstrate that the NAD/GI EDTA-WO_3/GCE possess excellent electrocatalytic activities towards the oxidation of NEP, MEL and NIC, which can be attributed to its unique structural features and excellent electrochemical properties. It was noted that the NAD immobilized, but non-irradiated EDTA-WO_3/GCE, also did not give the desired results indicating that the combination of NAD and gamma irradiation on EDTA-WO_3 have contributed to the significant simultaneous sensing of three important biomolecules.

The analytical parameters for the simultaneous detection of NEP, MEL and NIC using NAD/GI EDTA-WO_3 modified GCE have been optimized in terms of different scan cycles (3–30 cycles) of NAD electro-deposition and different concentrations of WO_3 NPs. As shown in Fig. 2B, the maximum peak currents of NEP, MEL and NIC were obtained at the optimized scan cycles of 18. In higher scan cycles, the peak currents decreased as the prolonged deposition produce thicker film, which in turn, would hinder electron transfer between the electrode surface and the bulk solution. Therefore, the scan cycles of 18 was found to be the optimal parameter for the electro-deposition of NAD. The varying amount of WO_3 NPs concentrations ranging from 1.0 to 10.0 mg/mL on the NAD immobilized electrode tended to a limiting value of peak currents of the analytes. As shown in Fig. 2C, the peak current responses of NEP, MEL and NIC increased with increasing the amounts of WO_3 NPs until 5.0 mg/mL and subsequently decreased with further increase in WO_3 NPs (< 5.0 mg/mL). The observed behavior

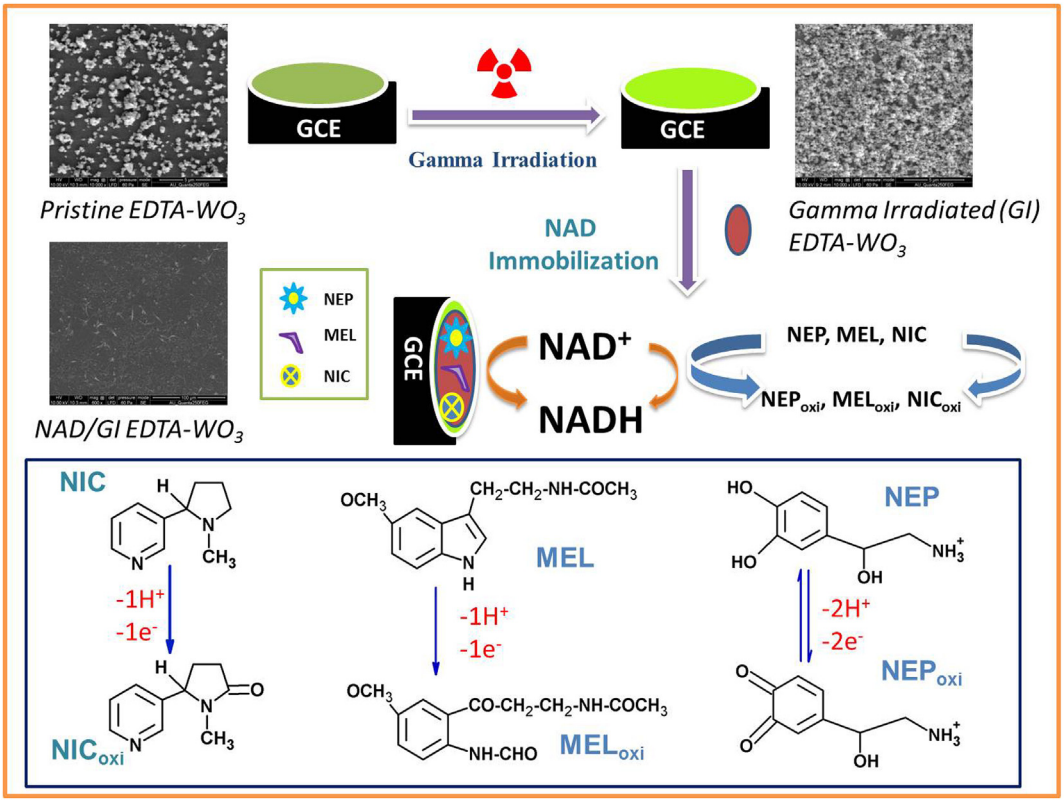

Scheme 1. Plausible mechanism of the simultaneous determination of NEP, MEL and NIC at NAD/GI EDTA-WO_3/GCE in 0.1 M PBS (pH 7.0).

could be due to the fact that the higher amount of WO_3 NPs enhances interface electron transfer resistance, changes electrode surface area and reduces the density of NAD. Therefore, the optimum WO_3 NPs content was chosen as 5.0 mg/mL for all the subsequent measurements.

The pH influence on the peak currents of NEP, MEL and NIC on NAD/GI EDTA-WO_3/GCE was investigated by CV method at various pH values in 0.1 M PBS. As shown in Fig. 2D, the modified electrode shows electrocatalytic activity over a wide range of pH (4.0–10.0), but higher peak currents of all the three analytes were observed at neutral pH 7.0. This pH (7.0) value was applied in subsequent experiments.

The detailed oxidation mechanism is shown in Scheme 1. The enzymatically active regeneration of 1,4-NADH on WO_3 led to the increase of oxidation current of NEP, MEL and NIC. NEP contains catechol residue and a side-chain amine group which are capable of forming norepinephrinequinone due to oxidation reaction. The electrochemical process of MEL involves the formation of cation at 5-position of the indole ring to form N-acetyl-N-formyl-5- methoxykynuramine due to transfer of two electrons and one proton. The oxidation mechanism of NIC involves the formation of methanol and substitution of the CH_3 to OH in the tertiary nitrogen of pyrrolidine ring with two electron transitions.

3.3. Simultaneous and individual determination of NEP, MEL and NIC on NAD/GI EDTA-WO_3/GCE

SWV measurements were performed in 0.1 M PBS (pH 7.0) in the potential region from −0.2–1.4 V with amplitude of 50 mV, frequency of 10 Hz and quiet time of 2 s. Fig. 3A–C shows SWV response of all the three analytes. Measurements were made for various concentration of one substance while keeping the other two constants. In case of NEP, the oxidation peak current increased proportionally with increase in its concentration from 0.010 μM to 1000 μM at the fixed amounts of MEL (75 μM) and NIC (25 μM). A linear regression equation between the I_{pa} with C_{NEP} was obtained as I_p (μA) = 1.163 + 0.625 C_{NEP} (0.010–100 μM) (R^2 = 0.9991) and I_p (μA) = 53.6 + 0.054 C_{NEP} (100–1000 μM) (R^2 = 0.9996). The detection limit for NEP was calculated to be 0.0014 μM. Similarly, the concentrations of NEP and NIC at 15 μM and 25 μM respectively were kept constant; the concentration of MEL was changed within the range of 0.010–1000 μM. The linear regression equation of MEL was deduced as I_p (μA) = 0.589 + 0.221 C_{MEL} (0.010–100 μM) (R^2 = 0.9981) and I_p (μA) = 19.9 + 0.020 C_{MEL} (100–1000 μM) (R^2 = 0.9989). The detection limit for MEL was calculated to be 0.0026 μM. In the same way, the concentration of NEP and MEL were retained as constant at 15 μM and 75 μM respectively, and the concentration range of NIC was varied from 0.010 to 1000 μM; the linear regression equation of NIC was deduced as I_p (μA) = 1.722 + 0.331 C_{NIC} (0.010–100 μM) (R^2 = 0.9986) and I_p (μA) = 30.12 + 0.049 C_{NIC} (100–1000 μM) (R^2 = 0.9992) and the detection limit for NIC was 0.0017 μM. All these measurements were performed under signal-to-noise ratio of S/N = 3. These experimental results indicated that the simultaneous determination of the above three species is feasible in mixture solution using SWV response. As shown in Fig. 3D, three oxidation peaks were well separated, and the peak currents increased in proportion to their concentrations from 0.010 to 1000 μM without affecting the peak potential and current of any analyte presented in Fig. 3A, B and C. The observed results demonstrate that the individual and simultaneous determination of the three analytes were in the same concentration range, but not interfering with one another, which indicates the highly selective nature of the sensor towards chosen analyte(s).

In order to make a comparison with recently reported sensors, the characteristics of different electrochemical sensors for NEP, MEL and NIC determination are summarized in Table 1. It can be seen that the fabricated sensor offered simultaneous detection of NEP, MEL and NIC for the first time, with wide linear ranges and lowest detection limits compared with that of most sensors reported for individual detection of NEP, MEL and NIC analytes. The significant improvement in the detection limit over a wide concentration range of NEP, MEL and NIC

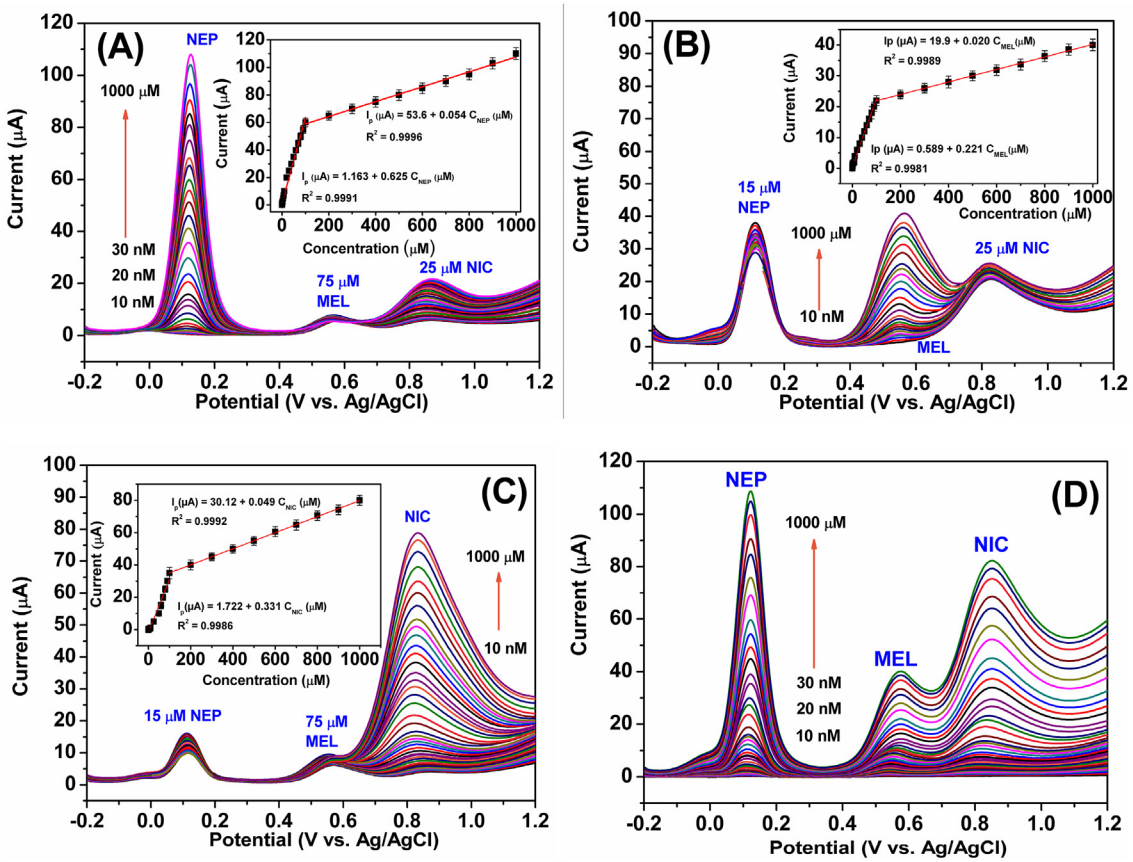

Fig. 3. SWVs profiles of NAD/GI EDTA-WO_3/GCE in 0.1 M PBS (pH 7.0) at different concentrations (0.010–1000 µM) of individual NEP (A), MEL (B), NIC (C) and (D) the simultaneous determination of NEP, MEL and NIC with increasing concentrations from 0.010 to 1000 µM; Inset of (A), (B) and (C) shows the corresponding plots of the anodic peak current vs. concentrations for NEP, MEL and NIC, in which the maximum relative standard deviations (RSDs) reach 3.24%, 2.16% and 2.43% for individual determination for NEP, MEL and NIC.

could be attributed to the fact that the NAD/GI EDTA-WO_3 possesses high electroactive surface area, unique morphology, high oxygen vacancies and good electrocatalytic activity.

3.4. Interference, stability and reproducibility studies of the modified electrode

Under the optimal experimental conditions, the influence of various potentially interfering agents existing in pharmaceuticals and cigarette samples on the determination NEP, MEL and NIC was investigated. Fig. S4 shows the anti-interference ability of the NAD/GI EDTA-WO_3/GCE towards the simultaneous determination of NEP, MEL and NIC in 0.1 M PBS (pH 7.0). The influence of 500-fold excess of ADP, ATP, glucose, folic acid, tyrosine, tryptophan, uric acid, cysteine, ascorbic acid, metal ions such as Na^+ ions, K^+ ions and 50-fold excess of dopamine, serotonin, epinephrine, cotinine and guanine were tested on the SWV response in the presence of 5 µM each of NEP, MEL and NIC. The tolerance limit was defined as the maximum concentration of the interfering substance that caused approximately 5% relative error in the simultaneous determination of NEP, MEL and NIC. There is no significant shift in the oxidation peak currents and peak potentials recorded in the presence of the interfering species indicating that the NAD/GI EDTA-WO_3/GCE can be considered as a good electrochemical biosensor for the recognition of NEP, MEL and NIC simultaneously in aqueous solutions with good anti-interference property.

The long-term stability and reproducibility of NAD/GI EDTA-WO_3/GCE have been evaluated by SWV technique. The stability of the proposed electrode was evaluated at 10 µM concentration of each analyte

Table 1
Comparison of the fabricated sensor with the NEP, MEL and NIC sensors reported in the literature.

Electrode	Linear Range (µM)			Detection limit (µM)			Ref.
	NEP	MEL	NIC	NEP	MEL	NIC	
$FeMoO_4$/GCE	1–200			0.0037			Samdani et al. (2016)
WO_3–TiO_2/ITO	3.23–388			1.07			Li et al. (2012)
MWCNT/ZnO/chitosan/SPE	0.5–30			0.2			Wang et al. (2015)
SnO_2–Co_3O_4/rGO/IL/CPE		0.02–6			0.0041		Zeinali et al. (2017)
N-doped graphene/$CuCO_2O_4$/CPE		0.01–3			0.0049		Tadayon and Sepehri, 2015
Gr/Fe_3O_4/CPE		0.02–5.80			0.0084		Bagheri et al. (2015)
TiO_2/PEDOT/MIP			0–5000			4.9	Wu et al. (2009)
Nano TiO_2/CPE			2–540			0.0134	Shehata et al. (2016)
ZnO/graphene nanofibers			0–10			0.074	Tabassum and Gupta, 2017
NAD/GI-EDTA WO_3	**0.01–1000**	**0.01–1000**	**0.01–1000**	**0.0014**	**0.0026**	**0.0017**	**Present work**

Table 2
Determination of NEP, MEL and NIC in commercial samples and comparison of the proposed method with other methods.

Samples	Analyte	Addition (μM)	Found (μM)	RSD (%)	Recovery (%)	Reference method
NEP injection	NEP	0	6.24	2.33	–	6.03
		3	9.32	4.32	100.32	9.14
		6	12.04	3.70	101.25	11.98
MEL tablet	MEL	0	0.85	2.56	–	0.79
		0.5	1.44	3.21	98.63	1.30
		1.0	1.85	2.89	99.29	1.83
Cigarette sample	NIC	0	5.17	2.33	–	4.92
		5	10.43	1.98	99.54	9.93
		10	15.23	3.04	101.34	14.87

in a solution over a period of 30 days at pH 7.0. It was found that the peak currents of NEP, MEL and NIC remained unchanged for the first 20 days with relative standard deviation (RSD) as ± 1.54%, ± 1.96%, and ± 1.72%. After 20 days, a deviation in the peak current was noticed with increase in variations in RSD values, therefore it is concluded that the sensor can be successfully used for the first 20 days. The reproducibility of the proposed approach was evaluated by intra- and inter-assay coefficients of variation. The intra-assay precision of this method was evaluated by assaying 10 μM each of NEP, MEL and NIC for six replicative measurements using the same NAD/GI EDTA-WO_3/GCE (Fig. S5A), and the inter-assay precision was evaluated by assaying 10 μM concentration of each analyte (NEP, MEL and NIC) in 0.1 M PBS (pH 7.0) for successive measurements using six modified electrodes made independently (Fig. S5B). The relative standard deviations (RSD) values for intra-assay were observed as ± 0.45%, ± 0.74% and ± 0.52% for NEP, MEL and NIC respectively, while the inter-assay RSDs were ± 0.63% (NEP), ± 0.86% (MEL) and ± 0.78% (NIC). These results indicated the NAD/GI EDTA-WO_3 modified GCE biosensor held satisfactory performances in stability and reproducibility, and it would be applicable for the analysis of real samples.

3.5. Analysis of real samples using NAD/GI EDTA-WO_3/GCE

The practical application of NAD/GI EDTA-WO_3 modified GCE was tested by measuring the concentration of NEP in norepinephrine bitartrate injection, MEL in melatonina tablet and NIC in cigarette samples. The standard addition technique was used for the determination of these analytes and the analytical results are listed in Table 2. Satisfactory recovery of the experimental results was found for NEP, MEL and NIC which indicates that the method could be efficiently used for the determination of NEP, MEL and NIC in commercial samples and compared with the reference method (Zhang and Stewart, 1993; Zeinali et al., 2017; Svorc et al., 2014).

4. Conclusions

In the present work, a novel biosensor was developed, for the first time, based on the nicotinamide adenine dinucleotide (NAD) immobilized gamma ray irradiated EDTA-WO_3 nanoparticles modified glassy carbon electrode (NAD/GI EDTA-WO_3/GCE) for the simultaneous detection of norepinephrine, melatonin and nicotine. Square wave voltammetry was found to be more suitable technique for the electrocatalytic determination of NEP, MEL and NIC in the presence of several potential interfering physiological biomolecules. Remarkably, the lowest detection limits of 1.4 nM, 2.6 nM and 1.7 nM have been obtained for determination of NEP, MEL and NIC respectively, either individually or simultaneously over a wide dynamic range of 0.010–1000 μM in 0.1 M PBS (pH 7.0). Furthermore, the proposed biosensor could be successfully applied in commercial samples (injection, tablets and cigarette) for the determination of NEP, MEL and NIC with good stability and excellent reproducibility. Future work may include further optimization of the biosensor, developing integrated sensing system and expanding its application to monitor the biomolecules in vivo.

Declaration of competing interest

The authors declare that they have no known competing financial interests or personal relationships that could have appeared to influence the work reported in this paper.

Conflicts of interest

We wish to confirm that there are no known conflicts of interest associated with this publication and there has been no significant financial support for this work that could have influenced its outcome.

CRediT authorship contribution statement

A.C. Anithaa: Data curation, Methodology, Writing - original draft. **K. Asokan:** Visualization, Supervision. **N. Lavanya:** Investigation, Validation. **C. Sekar:** Conceptualization, Supervision, Writing - review & editing.

Acknowledgements

The authors acknowledge the DST (SERB–SB/S2/LOP-027/2013; SR/PURSE Phase 2/38 (G) dated:21.02.2017) and MHRD-RUSA 2.0 (No. F.24-51/2014- U, Policy (TNMulti-Gen), dated .09.10.2018) for the financial assistance.

Appendix A. Supplementary data

Supplementary data to this article can be found online at https://doi.org/10.1016/j.bios.2019.111598.

References

Akhtar, M.H., Hussain, K.H., Gurudatt, N.G., Chandra, P., Shim, Y.B., 2018. Biosens. Bioelectron. 116, 108–115.
Alejandra, T., Roberto, C., Maria, J.M., Humberto, G., 2016. Bioconjug. Chem. 27, 2581–2591.
Ali, I., Soomro, B., Omanovic, S., 2011. Electrochem. Commun. 13, 562–565.
Anithaa, A.C., Lavanya, N., Asokan, K., Sekar, C., 2015. Electrochim. Acta 16, 294–302.
Anithaa, A.C., Asokan, K., Sekar, C., 2017a. Sens. Actuators B Chem. 238, 667–675.
Anithaa, A.C., Asokan, K., Sekar, C., 2017b. Electrochim. Acta 237, 44–53.
Anithaa, A.C., Asokan, K., Sekar, C., 2017c. Sens. Actuators B Chem. 247, 814–822.
Anithaa, A.C., Asokan, K., Sekar, C., 2018. J. Taiwan Inst. Chem. Eng. 84, 11–18.
Ardakani, M.M., Beitollahi, H., Amini, M.K., Mirkhalaf, F., Alibeik, M.A., 2010. Sens. Actuators B Chem. 151, 243–249.
Bagheri, H., Afkhami, A., Hashemi, P., Ghanei, M., 2015. RSC Adv 5, 21659–21669.
Goyal, R.N., Aziz, M.A., Oyama, M., Chatterjee, S., Rana, A.R.S., 2011. Sens. Actuators B Chem. 153, 232–238.
Kumar, N., Rosy, Goyal, R.N., 2016. Electrochim. Acta 211, 18–26.
Lee, W.C., Noh, H.B., Hussain, K.H., Min, S.J., Shim, Y.B., 2018. Sens. Actuators B Chem. 275, 284–291.
Levent, A., 2012. Diam. Relat. Mater. 21, 114–119.
Li, Y., Hsu, P.C., Chen, S.M., 2012. Sens. Actuators B Chem. 174, 427–435.
Meng, T., Zheng, Z.H., Liu, T.T., Lin, L., 2012. Neurochem. Res. 37, 1050–1056.

Samdani, K.J., Samdani, J.S., Kim, N.H., Lee, J.H., 2016. Biosens. Bioelectron. 81, 445–453.
Shehata, M., Azab, S.M., Fekry, A.M., Ameer, M.A., 2016. Biosens. Bioelectron. 79, 589–592.
Svorc, L., Stankovic, D.L., Kalcher, K., 2014. Diam. Relat. Mater. 42, 1–7.
Tabassum, R., Gupta, B.D., 2017. Biosens. Bioelectron. 91, 762–769.
Tadayon, F., Sepehri, Z., 2015. RSC Adv. 5, 65560–65568.
Thomas, J., Khanam, R., Vohora, D., 2015. Pharm. Biol. 53, 1539–1544.
Vargas, H.O., Nunes, S.O., Castro, M.R., Vargae, M.M., Barbosa, D.S., Bortolasci, C.C., Venugopal, K., Doss, S., Berk, M., 2013. Neurosci. Lett. 544, 136–140.
Wang, Y., Wang, S., Tao, L., Min, Q., Xiang, J., Wang, Q., Xie, J., Yue, Y., Wu, S., Li, X., Ding, H., 2015. Biosens. Bioelectron. 65, 31–38.
Wang, Y., Zhang, B., Liu, J., Yang, Q., Cui, X., Gao, Y., Chuai, X., Liu, F., et al., 2016. Sens. Actuators B Chem. 236, 67–76.
Wu, C.T., Chen, P.Y., Chen, J.G., Suryanarayanan, V., Ho, K.C., 2009. Anal. Chim. Acta 633, 119–126.
Yang, Y., Xie, R., Liu, Y., Li, J., Li, W., 2015. Catalysts 5, 2024–2038.
Yasuda, M., Ota, T., Morikawa, A., Mawatari, K., Fukuuchi, T., Yamaoka, N., Kaneko, K., Nakagomi, K., 2013. J. Chromatogr. B 934, 41–45.
Zeinali, H., Bagheri, H., Khoshhesab, Z.M., Khoshsafar, H., Hajian, A., 2017. Mater. Sci. Eng. C Mater. Biol. Appl. 71, 386–394.
Zhang, H., Stewart, J.T., 1993. J. Liq. Chromatogr. 16, 2861–2871.
Zhang, T., Zhu, Z., Chen, H., Bai, Y., Xiao, S., Zheng, X., Xue, Q., Yang, S., 2015. Nanoscale 7, 2933–2940.